

Numerical investigation of effects of rotating downdraft on tornado-like-vortex characteristics

Shuyang Cao¹, Mengen Wang², Jinwei Zhu³, Jinxin Cao^{*1}, Tetsuro Tamura⁴ and Qingshan Yang⁵

¹State Key Lab of Disaster Reduction in Civil Engineering, Tongji University, Shanghai 200092, China

²College of Civil Engineering, Tongji University, Shanghai 200092, China

³Shanghai Urban Construction Design & Research Institute Shanghai, China

⁴Tokyo Institute of Technology, Japan

⁵Chongqing University, China

(Received October 18, 2017, Revised December 22, 2017, Accepted December 29, 2017)

Abstract. Appropriate modeling of a tornado-like vortex is a prerequisite when studying the near-ground wind characteristics of a tornado and tornado-induced wind loads on structures. Both Ward- and ISU-type tornado simulators employ guide vanes to induce angular momentum to converge flow in order to generate tornado-like vortices. But in the Ward-type simulator, the guide vanes are mounted near the ground while in the ISU-type they are located at a high position to allow vertical circulation of flow that creates a rotating downdraft to generate a tornado-like vortex. In this study, numerical simulations were performed to reproduce tornado-like vortices using both Ward-type and ISU-type tornado simulators, from which the effects of rotating downdraft on the vortex characteristics were clarified. Particular attention was devoted to the wander of tornado-like vortices, and their dependences on swirl ratio and fetch length were investigated. The present study showed that the dynamic vortex structure depends significantly on the vortex-generating mechanism, although the time-averaged structure remains similar. This feature should be taken into consideration when tornado-like-vortex simulators are utilized to investigate tornado-induced wind forces on structures.

Keywords: Tornado-like vortex; large-eddy simulation; vortex wander; rotating downdraft

1. Introduction

Tornadoes are strong vortices with high wind speeds that may cause severe damage to structures. Due to the extremely low probability of a building being hit by a tornado, there have been very few studies on tornado loads in countries such as China and Japan that have not been considered as tornado-prone countries. However, in the past two decades, the incidence of tornadoes has increased in Asia (Tamura *et al.* 2007, Cao and Wang 2013), possibly due to global climate change. This has had a significant impact on society, and has motivated a lot of tornado-related studies.

It is essential to understand the wind characteristics of a tornado near the ground and tornado-structure interaction when investigating tornado-induced wind loads on structures. Physical simulations of a tornado started with Chang (1971), who generated tornado-like vortices with a rotating cylindrical screen, and subsequently with Ward (1972), who modeled tornado-like flow by mounting a fan above the test area to provide an updraft, and guide vanes around the test area to generate swirling flow. Ward's device assumed that the vortex structure near the ground was mainly governed by the mechanical supply of angular momentum, and now it is referred to as a Ward-type tornado simulator. Many experimental studies have utilized a Ward-

type simulator to investigate a tornado-like vortex and its effects on structures (Church *et al.* 1979, Sabareesh *et al.* 2013). Meanwhile, Haan *et al.* (2008) constructed a large tornado vortex simulator at Iowa State University, USA, also for wind engineering applications, which was a modification of the Ward-type tornado vortex simulator. In this simulator, the guide vanes are located at a high position to allow vertical circulation of flow in the process of generating a tornado-like vortex. The rotating downdraft mechanism it offered was considered advantageous for modeling the rear flank downdraft phenomenon of a real tornado. It also enables modeling of the translational motion of a tornado, making it attractive to structural engineers who are interested in tornado effects on structures. This relatively new type of tornado simulator, referred to as an ISU-type simulator hereafter, has recently been utilized to investigate tornado-induced loads on low-rise and high-rise structures (Haan *et al.* 2010, Kikutsu *et al.* 2010, Cao *et al.* 2015). On the other hand, as a powerful tool for providing three-dimensional flow information, Computational Fluids Dynamics (CFD) methods have also been widely utilized to model a tornado-like vortex in order to study tornado-induced wind forces on building models. Both Reynolds Averaged Navier-Stokes (RANS) equation simulation (for example Kuai *et al.* 2008) and Large Eddy Simulation (LES) (Lewellen *et al.* 1997, Natarajan and Hangan 2012, Liu and Ishihara 2015) have been used to calculate the time-averaged velocity and pressure features that were the main concerns of simulations. However, the majority of previous numerical simulations used the Ward-type simulator, and

*Corresponding author, Assistant Professor
E-mail: jinxin@tongji.edu.cn

simulation using ISU-type tornado simulators has seldom been tried. Although these two types of simulator currently co-exist for wind engineering application, the differences between the tornado-like vortex characteristics they produce are not well understood due to the limited number of experimental and numerical studies. Wang *et al.* (2017a) noticed inconsistencies among the results of roughness effects on tornado-like vortices reported by different researchers and doubted that they were caused by different tornado-generation mechanisms in their experimental facilities, i.e., with/without rotating downdraft. Insufficient understanding of tornado-like vortex structure will inevitably hinder physical explanations of tornado-induced wind loads on structures. Thus, it is critical to clarify the time-averaged and instantaneous vortex structures and their variations with vortex-generating mechanism.

Swirl ratio, which is defined as the ratio of angular momentum to radial momentum in a vortex, is known to be a dominant non-dimensional parameter in determining tornado flow pattern. However, other parameters such as aspect ratio, Reynolds number and Froude number also play non-negligible roles (Rotunno 1977, Church *et al.* 1979). One well-known feature of a tornado vortex is its single-cell or multiple-cell structure, whose dependence on swirl ratio has attracted a lot of attention in the past. Based on studies on the Ward-type simulator, Church (1979) and Monji (1985) showed that a tornado-like vortex is a single cell one, being laminar when swirl ratio is less than about 0.3 and turbulent when the swirl ratio is about 0.3-0.6. However, the vortex changes into two or three subsidiary vortices when swirl ratio is further increased. It is therefore desirable to consider several representative swirl ratios when studying the effects of a rotating downdraft. Reynolds number is also an important parameter to influence the tornado flow field. The swirl ratio associated with transition to multiple-cell structure depends on the radial Reynolds number. If Reynolds number is smaller, larger swirl ratio is needed to observe the transitions from single-cell to two-cell and two-cell to multiple-cell. However, the influence of Reynolds number on the vortex-like structure has been shown to be secondary to that of swirl ratio (Refan and Hangan 2017). Thus, the Reynolds number dependence of the simulation results is not considered in the present study. On the other hand, the length of fetch, which is the distance from the location of adding angular momentum to vortex center, may change the vortex characteristics. However, the influence of fetch length, to the author's knowledge, has never been studied. In summary, the previous studies on the tornado-like vortex characteristics are insufficient, and more researches on the differences in vortices modeled by different simulators are necessary.

In the present study, we carried out large-eddy simulations to reproduce tornado-like vortices with/without the contribution of a rotating downdraft first at two representative swirl ratios. The numerical results were compared with available experimental and field data to validate the adopted numerical method. Then the time-averaged and instantaneous vortex structures of the two types of simulator, especially vortex wander, were compared in order to clarify the effects of rotating

downdraft. In addition, the dependence of flow characteristics on fetch length was studied. The results of the present study are considered important not only for understanding tornado-induced wind loads on structures, but also for designing ISU-type tornado simulators.

2. Numerical method

2.1 Governing equations and numerical procedure

Time-dependent unsteady finite volume approximation was carried out to reproduce tornado-like vortices. The governing equations for the three-dimensional incompressible large-eddy simulation are the filtered continuity equation and Navier-Stokes equations expressed as

$$\frac{\partial \bar{u}_i}{\partial x_i} = 0 \quad (1)$$

$$\frac{\partial \bar{u}_i}{\partial t} + \frac{\partial}{\partial x_j} (\bar{u}_i \bar{u}_j) = -\frac{1}{\rho} \frac{\partial \bar{p}}{\partial x_i} + \frac{1}{\rho} \frac{\partial}{\partial x_j} \left(\mu \frac{\partial \bar{u}_i}{\partial x_j} \right) - \frac{1}{\rho} \frac{\partial \tau_{ij}}{\partial x_j} \quad (2)$$

where \bar{u}_i ($i=1, 2, 3$) and \bar{p} are the three filtered velocity components and pressure respectively, ρ is density, and τ_{ij} is the SGS stress. The principal idea of LES is to reduce the computational cost by directly resolving the grid scale turbulence while modeling the sub-grid-scale turbulence, via low-pass filtering of the governing equations of fluids. SGS stress can be modeled as

$$\tau_{ij} = \frac{1}{3} \delta_{ij} \tau_{kk} - 2\nu_e \bar{S}_{ij}, \quad \bar{S}_{ij} = \frac{1}{2} \left(\frac{\partial \bar{u}_i}{\partial x_j} + \frac{\partial \bar{u}_j}{\partial x_i} \right) \quad (3)$$

where ν_e is the subgrid-scale turbulent viscosity, \bar{S}_{ij} is the rate-of-strain tensor for the resolved scale, and δ_{ij} is the Kronecker delta. The Smagorinsky-Lilly SGS model is used to calculate turbulent viscosity (Ishihara *et al.* 2011).

An open source solver OpenFOAM is used to solve the governing equations, and the options it offers for simulation are carefully selected in order to achieve reliable results.

The second-order central difference scheme is used for both convection and diffusion terms. The PIMPLE algorithm, which combines SIMPLE (Semi-Implicit Method for Pressure-Linked Equations) and PISO (Pressure Implicit with Splitting of Operators) algorithms, is used to solve the discretized equations. The SIMPLE algorithm is utilized, in which governing equations are solved sequentially because of their non-linearity and coupling characteristics and the solution loop is carried out iteratively in order to obtain a converged numerical solution. The pressure field is extracted by solving a pressure correction equation obtained by manipulating continuity and momentum equations, while the velocity field is obtained

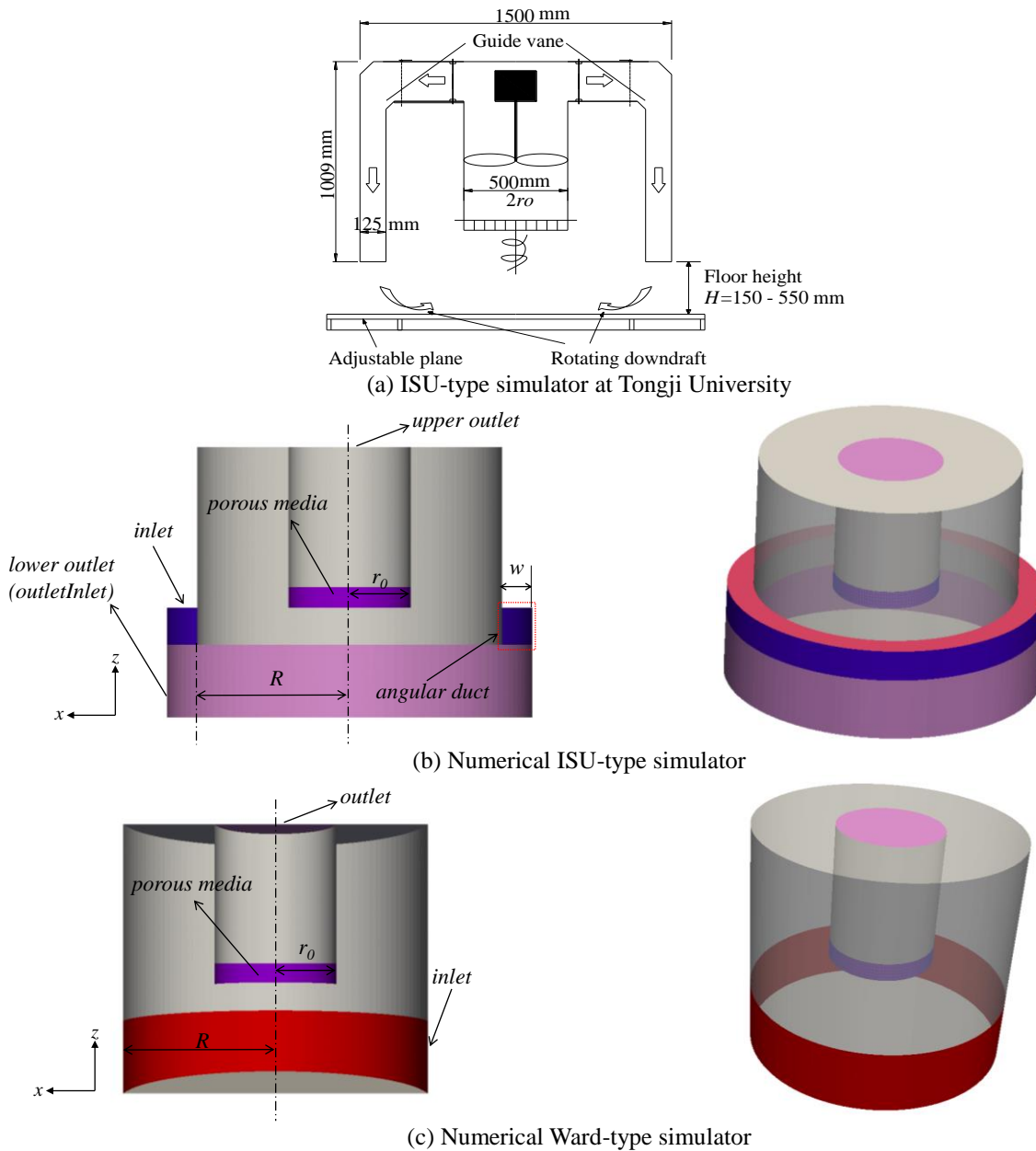


Fig. 1 Schematic diagram of physical and numerical tornado simulators

from the momentum equations. In addition, the convergence criteria of the iterative calculation are set to 1×10^{-7} for velocity and 1×10^{-5} for pressure, respectively. Meanwhile, a fully implicit second-order time-advancement scheme is chosen for temporal discretization to obtain stable and accurate simulation.

2.2 Numerical model, grid system and boundary conditions

An ISU-type tornado-like-vortex simulator constructed at Tongji University, China (Wang *et al.* 2017a) is utilized as the prototype for simulation. As shown in Fig. 1(a), the physical simulator has a circular duct 1.5 m in diameter and 1.0 m in height, which is suspended overhead by a 0.5 m

diameter updraft holding a controlling fan to generate a strong updraft. A screen and a honeycomb below the fan are mounted at the center of the duct. In total, 18 guide vanes with adjustable orientation angle are placed at the top of the simulator equally spaced along the inner periphery of the annular duct to generate a rotating downdraft that causes a swirling flow. This ISU-type tornado-like-vortex simulator is numerically modeled in this study, in which an angular duct illustrated in Fig. 1(b) is set to introduce the rotating downdraft flow that was achieved by imposing boundary conditions of velocity instead of physical modeling of guide vanes. The numerical Ward-type simulator shown in Fig. 1(c) is geometrically the same as the ISU-type one except that the angular duct is removed.

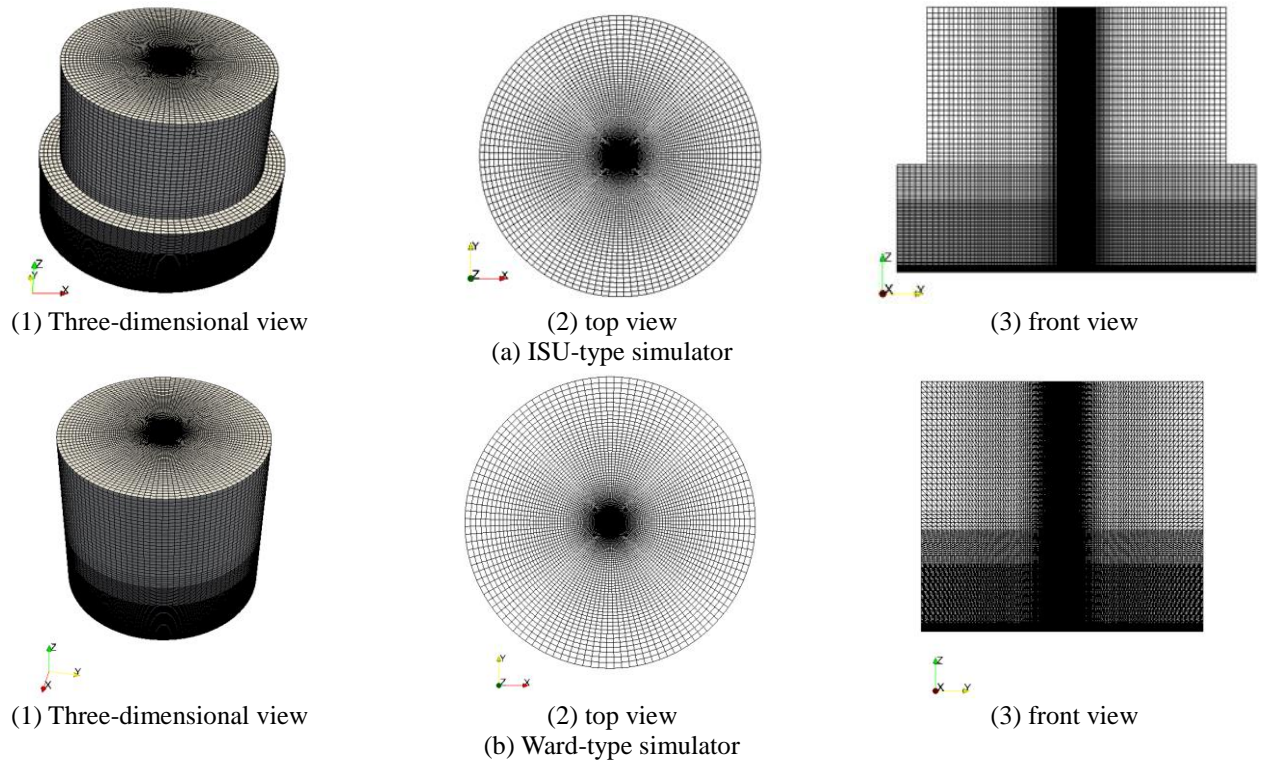


Fig. 2 Mesh systems of simulators

The role of the guide vanes is also achieved by imposing boundary conditions of velocity. It is noteworthy that the divider plate between convergence region and convection region of the original Ward-type simulator (Church *et al.* 1979) are not modelled because the present study aims at the effects of rotating downdraft. The main geometries of the two types of simulator are identical and equal to those of the prototype. The radius of the updraft hole r_0 is 0.250 m; the inflow height H is fixed at $H=0.3$ m as for the experiment of Wang *et al.* (2017a), resulting in an aspect ratio $a=H/r_0=1.2$. The confluence region radius R , which is the fetch needed to make the swirling flow converge, is 0.625m. The width w of the angular duct of the ISU-type simulator is 0.125 m.

The swirl ratio is calculated as the ratio of angular momentum to radial momentum in the vortex, which can be expressed as $S = \frac{\Gamma}{2Qa}$ (Church *et al.* 1979), where Γ is

the free-stream circulation at the outer edge of the convergence region, $\Gamma=2\pi R \int_0^H U_t dh$; H is the inflow

height; R is the radius of the convergence region; U_t is the mean tangential velocity at the corresponding position; and Q is the volume flow rate, which is calculated by integrating the vertical velocity at the outflow boundary. In the present study, the effect of rotating downdraft is investigated under two swirl ratios 0.15 and 0.74 corresponding to laminar and turbulent flow conditions suggested by Church (1979) and Monji (1985), respectively.

In order to maintain the swirl ratio almost unchanged when comparing the two types of simulator, the tangential

velocity at the inlet boundary of the simulators is adjusted. Another important parameter, Reynolds number, is defined as $Re=Q/H\nu$ (Matsui and Tamura 2009) in the present study, where Q is the flow rate through the simulator, H is the height of the inlet and ν ($14.8 \times 10^{-6} \text{ m}^2/\text{s}$) is the kinematic viscosity.

Because of the axisymmetric features of tornado-like vortices, an axisymmetric grid system is adopted for the simulation. As illustrated in Fig. 1, the computational domains of the two types of simulator are basically the same except that the ISU-type simulator has an angular duct while the Ward-type does not. Thus, their mesh features are similar except in the angular duct region. Figs. 2(a) and 2(b) display the mesh system for the simulations with and without the angular duct respectively. The structured grid systems are utilized for the whole simulation domain including the inner circle and updraft hole. As a preliminary simulation in the present study, three structured O-type grid systems with different resolutions were tested to examine the mesh dependence of the simulation. All mesh systems adopted a fine mesh in the convergence region in order to investigate the turbulent features. The minimum mesh sizes in both vertical and radial directions, which are near the ground and at the domain center, respectively, are the same for the three tested mesh systems. The value of y^+ of the first grid near the ground is less than 2. The three mesh systems have different grid stretching ratios, 1.2, 1.15 and 1.1, to avoid a sudden change in grid size. Because the simulation results of mean velocity profile for the three tested mesh systems did not exhibit significant differences, the mesh system with a grid stretching ratio of 1.15 with a

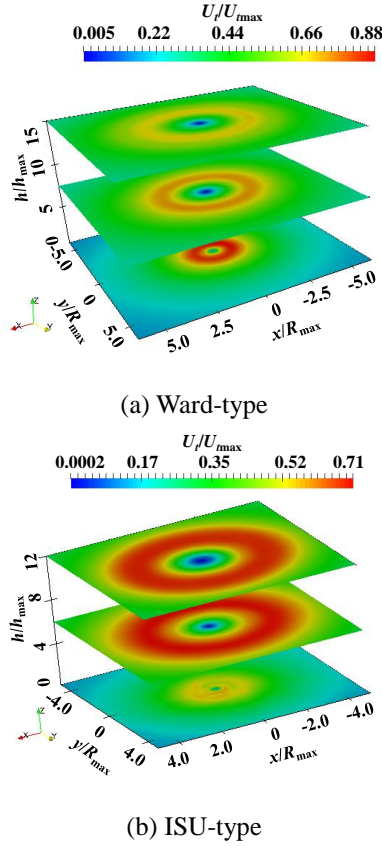


Fig. 3 Distribution of mean tangential velocity on horizontal planes at different heights

total of approximately 1.4 million grid cells is adopted in further calculations.

In the present study, the situations with/without rotating downdraft are achieved by imposing boundary conditions of velocity. For the Ward-type simulator without an angular duct, following Natarajan *et al.* (2012) and Liu and Ishihara (2015), the velocity profiles of $U_r = U(z/H)^{1/n}$, $U_t = -U_r \tan \theta$, are imposed at the inlet boundary, where U_r and U_t are radial and tangential velocities, respectively; U is the reference velocity at height H ; and θ is the inflow angle. Both radial and tangential velocities follow a power law distribution and the power law index is $1/7$, corresponding to a boundary layer developed on a smooth wall. The value of U is set as 0.52 m/s. The axial velocity is zero at the boundary. At the outlet boundary, a zero gradient condition is applied to the three velocity components. Different swirl ratios are obtained by altering the inflow angle θ . The location of the inlet boundary of the ISU-type simulator is different from that of the Ward-type simulator. The inlet is at the location of angular duct, and the inflow is composed of two velocity components, vertical axial velocity U_v (which is set to guarantee that the volume rate is the same as that for the case without the effect of rotating downdraft) and tangential velocity U_t .

The radial velocity at the inlet boundary is zero. The swirl ratio is changed by adjusting the value of U_t . There

are two outlet boundaries for the ISU-type simulator. At the upper outlet boundary, a zero gradient condition is applied to three velocity components, which is the same as Ward-type simulator. At the lower outlet boundary, a special “outletInlet” boundary condition that is specially designed by OpenFOAM for a boundary where the instantaneous flow direction is unknown is utilized. In particular, zero velocity boundary condition is imposed if the instantaneous flux is outward, and a zero-gradient velocity boundary condition is applied if the flux is inward. Porous media are applied in both simulation cases to achieve the honeycomb function, in which no drag force is added in the vertical momentum equation but almost infinite drag forces are added in the horizontal directions. Zero pressure gradient and zero pressure conditions are imposed at the inlet and outlet boundaries, respectively.

The simulation starts from rest. The total calculation time is 30s and the time step is $5e-04$ s. The initial transient effects disappear after 10s. All instantaneous and time-averaged flow features shown later are discussed based on the last 20s numerical results after the calculation becomes statistically steady. The averaging time 20s is about 300 ($S=0.74$, ISU type), 230 ($S=0.15$, ISU type), 400 ($S=0.74$, Ward type), 210 ($S=0.15$, Ward type) flow-through-domain times respectively. The quantitative analysis of vortex wander is based on 200 instantaneous flow snapshots that are extracted every 200 time steps (0.1s) from the time period of 20s to calculate the time-averaged velocity.

2.3 Validations

Due to the lack of sufficient laboratory and field data on tornado vortex structure, numerical simulation is validated by comparing the time-averaged flow fields. Detailed discussions on the transient, unsteady instantaneous field and the differences between with/without rotating downdraft, in other words, the dependences of tornado-like-vortex dynamics on the vortex-generation mechanism, are determined after validations.

Fig. 3 compares the spatial distribution of mean tangential velocity on the horizontal plane at different heights at swirl ratio $S=0.74$ obtained by Ward- and ISU-type simulators. Fig. 3 exhibits a typical horizontal velocity profile of a tornado, in which the tangential velocity increases with distance from the vortex center and decreases beyond the core radius. In addition, a funnel-shaped profile of mean velocity is illustrated in both Ward- and ISU-type simulators. Although both mean velocity profiles shown in Figs. 3(a) and 3(b) possess the basic vortex structures of a tornado-like vortex, they also indicate differences between the mean velocities and vortex core sizes produced by the two vortex-generating methods.

Fig. 4 compares the horizontal profile of tangential velocity at height $h/R_{\max} = 0.5$ (R_{\max} is the vortex core radius) obtained by the present numerical simulations for Ward- and ISU-type simulators, respectively, with comparisons with the experimental data of Wang *et al.* (2017a) and field measurement data of the Spencer and Mulhall tornadoes (Haan *et al.* 2008).

Table 1 Some important parameters of simulated tornado-like vortices

Simulation cases	R (m)	Swirl Ratio	Re	U_{tmax} (m/s)	R_{max} (m)	h_{max} (m)
ISU-type (with rotating downdraft)	0.425	0.80	1.2×10^5	4.65	0.062	0.019
	0.625	0.74	1.2×10^5	5.16	0.054	0.026
		0.15	1.2×10^5	1.79	0.024	0.033
	0.825	0.71	1.2×10^5	5.13	0.044	0.021
Ward-type (without rotating downdraft)	0.625	0.74	1.2×10^5	5.35	0.041	0.019
		0.15	1.2×10^5	1.53	0.023	0.020

The tangential velocities and distances to tornado-like-vortex center in Fig. 4 are normalized by the maximum tangential speed U_{tmaxh} at height $h/R_{max} = 0.5$ and the vortices radii R_{maxh} where U_{tmaxh} occurs, respectively. Both the present numerical simulations and the experiment of Wang *et al.* (2017a) were performed at same swirl ratio $S=0.74$, and the experimental results of both Wang *et al.* (2017a) and Haan *et al.* (2008) were obtained for an ISU-type simulator. Fig. 4 shows that all numerical, laboratory and field data exhibit a similar variation tendency of tangential velocity, i.e, the tangential velocity increases and decreases with distance from the vortex center inside and outside the vortex core, respectively, with a maximum tangential velocity at the vortex core radius. However, the swirl ratios and measurement heights for the simulation and field measurement were different. It can also be found that, despite the differences in the values of tangential velocity and core size produced by the Ward- and ISU-types simulators as shown in Fig. 3, the normalized profiles agree with each other, as well as with the laboratory and field data. In conclusion, the numerical models utilized to simulate the tornado-like vortices with/without the effect of rotating downdraft in the present study are considered to simulate

the typical statistical features of a tornado-like vortex such as the spatial funnel structure and mean velocity profiles with satisfactory accuracy, so they are considered applicable for further studies on the effects of rotating downdraft.

3. Results and discussions

In order to clarify the effects of rotating downdraft, two categories of simulation are conducted: with/without rotating downdraft. Each category contains two swirl ratios, $S=0.15$ and 0.74 , at a constant fetch length $R=0.625$ m. In addition, the simulations are performed at other two fetch lengths for ISU type simulator to study the effects of fetch length. Table 1 summarizes some important parameters that describe the configuration of a tornado-like vortex: swirl ratio S , Reynolds number Re , maximum tangential velocity U_{tmax} , vortex core radius R_{max} and height h_{max} where U_{tmax} occurs. It can be seen that the vortex core radius R_{max} increases with increase in swirl ratio for both ISU- and Ward-type simulators. However, the height of the maximum tangential velocity varies with the swirl ratio for the ISU-type simulator, while the elevation for maximum tangential velocity remains almost unchanged with swirl ratio for the Ward-type simulator.

3.1 Mean structure

Fig. 5 compares the horizontal profiles of tangential velocity at heights $h/R_{max} = 0.5$ and $h/R_{max} = 1.0$ at $R=0.625$ m. The radial distance to the vortex center is normalized by the core radius R_{maxh} , and the tangential velocity is normalized by the maximum tangential velocity U_{tmaxh} at the corresponding height. The tangential velocity profile of the ISU-type simulator coincides well with that of the Ward-type simulator at both heights at swirl ratio $S=0.74$, especially outside the vortex core. However, the tangential velocity profiles are distinctly different at swirl ratio $S=0.15$.

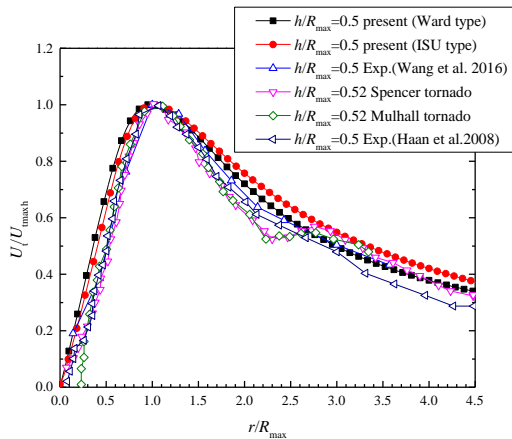


Fig. 4 Comparison among tangential velocity profiles of numerical, experimental and field data

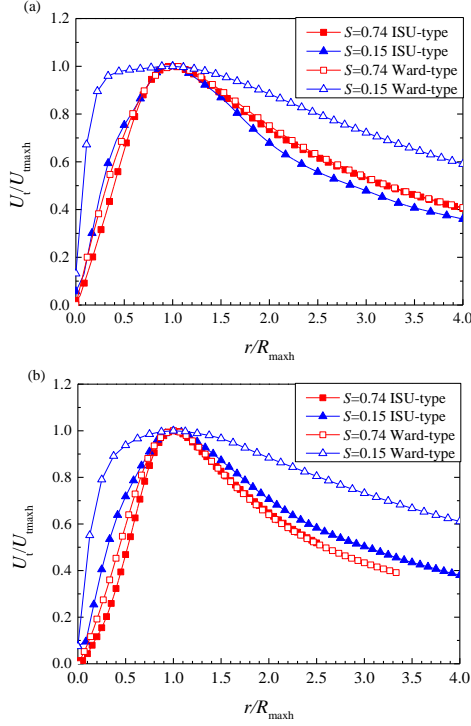


Fig. 5 Comparison of tangential velocity profile at two elevations, (a) $h/R_{\max}=0.5$ and (b) $h/R_{\max}=1.0$

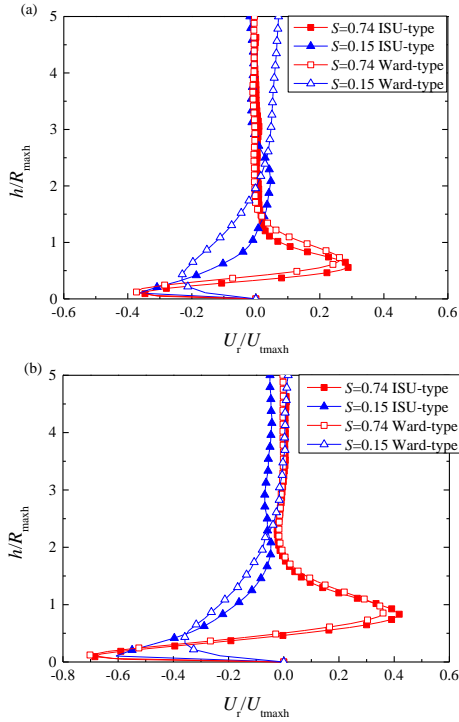


Fig. 6 Comparison of vertical profile of radial velocity, (a) $h/R_{\max}=0.5$ and (b) $h/R_{\max}=1.0$

The normalized mean tangential velocity at $S=0.15$ for the Ward-type simulator is obviously greater than that for the ISU-type simulator at both heights, and remains almost unchanged around the vortex core radius at the lower height

$h/R_{\max} = 0.5$.

Fig. 6 shows the vertical profile of radial velocity at two radial locations at different distances from the vortex center: inside the core ($r/R_{\max} = 0.5$) and at vortex radius ($r/R_{\max} = 1.0$). Positive and negative radial velocities imply outward and inward velocity, respectively. The radial velocity and height in Fig. 6 are normalized by the maximum tangential velocity $U_{t\max h}$ and the core radius $R_{\max h}$ of the corresponding simulation, respectively. It can be seen by comparing Fig. 6(a) with Fig. 6(b) that the radial velocity is greater at the vortex radius ($r/R_{\max} = 1.0$) than inside the vortex ($r/R_{\max} = 0.5$). A significant feature shown in Fig. 6 is that the radial velocity exhibits different variations with height at different swirl ratios. The radial velocities obtained by four simulations are negative near the ground, indicating that the flow moves toward the center of the tornado-like vortex. However, the inward flow changes to outward (positive) flow at heights greater than $0.5R_{\max}$ at $S=0.74$, although it remains inward at heights less than about $2R_{\max}$ when $S=0.15$.

The change of wind direction from inward to outward with increase in height at a high swirl ratio was also seen in laboratory experiments and field measurements (Kuai *et al.* 2008). With regard to the effects of rotating downdraft, the radial velocities are almost the same with the two types of simulator at high swirl ratio $S=0.74$, but are different at low swirl ratio $S=0.15$. The radial velocity is smaller for the Ward-type simulator at lower elevations at $S=0.15$.

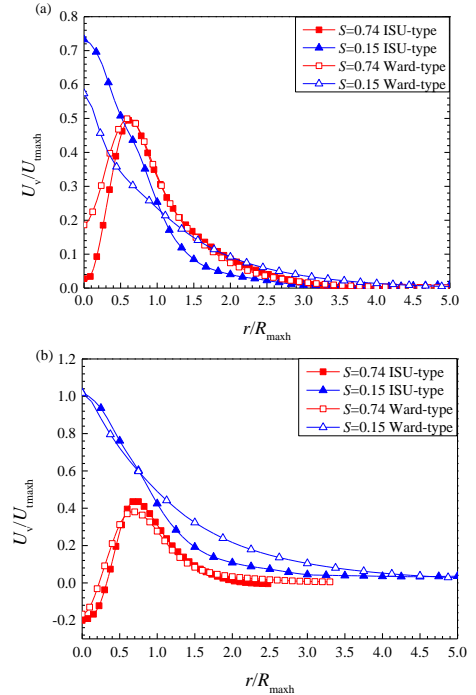


Fig. 7 Comparison of horizontal profile of axial velocity at two heights, (a) $h/R_{\max}=0.5$ and (b) $h/R_{\max}=1.0$

Fig. 7 compares the horizontal profile of axial velocity U_v at heights $h/R_{\max}=0.5$ and $h/R_{\max}=1.0$. The positive and negative values represent upward and downward winds, respectively. The axial velocity firstly increases and then decreases with radial distance at $S=0.74$ and its maximum value occurs at a location inside the vortex core at both heights. However, interestingly, the axial velocity changes from upward to downward at the tornado-like-vortex center at height $h/R_{\max}=1.0$. This implies that the flow at this elevation and above becomes turbulent. From the Fig. 7(a), no downdraft is observed which means that the laminar jet still exists and two-celled or multi-celled structure does not appear. However, the axial velocity remains positive (upward) while it decreases with distance to the tornado center. With regard to the effect of rotating downdraft, the Ward- and ISU-type simulators produce quite similar horizontal profiles of axial velocity outside the vortex core at $S=0.74$. However, those inside the core vary considerably at both heights. On the other hand, the rotating downdraft has a significant influence on the horizontal profile of axial velocity at $S=0.15$.

Fig. 8 compares the horizontal profile of mean pressure coefficients C_p obtained from the simulations with/without rotating downdraft. The pressure coefficient C_p is calculated by using static pressure at the inlet as the reference pressure and the maximum tangential velocity $U_{t\max}$ as the reference velocity. All simulations present a minimum pressure coefficient at the vortex center, and the pressure drop is bigger at $S=0.15$ than at $S=0.74$. Simulations with/without rotating downdraft show a sharp pressure drop with approximately equal minimum value at the tornado center at $S=0.15$, which implies that the rotating downdraft has little influence on the mean pressure coefficient. However, the horizontal profile of pressure drop becomes flat around the tornado center for both Ward- and ISU-type simulators at $S=0.74$, indicating an almost constant pressure drop within the tornado center. The flat distribution of pressure drop at $S=0.74$ is caused by the two-cell or multiple-cell vortex structure at the high swirl ratio, which was also reported by Haan *et al.* (2008) and Wang *et al.* (2017a). Fig. 8 shows that the maximum pressure drop inside the tornado core with rotating downdraft is less negative than without rotating downdraft. The pressure drop accompanying the tornado significantly affects the wind pressure acting on the structure surfaces (Wang *et al.* 2017b). Thus, the experimental results of tornado-induced pressure on structures may differ with the type of tornado simulator. This will cause difficulties in harmonizing model test results obtained with different tornado simulators.

Fig. 9 compares the horizontal profiles of standard deviation (STD) of tangential velocity $U_{t,\text{STD}}$ at two heights $h/R_{\max}=0.5$ and $h/R_{\max}=1.0$. It can be seen that, when swirl ratio $S=0.74$, the rotating downdraft has comparatively little and great influences on the STD of tangential velocity outside and inside the vortex core, respectively, at $h/R_{\max}=1.0$, whereas it has a strong effect at the lower height $h/R_{\max}=0.5$. The STD of tangential velocity of the

ISU-type simulator is much larger than that of the Ward-type tornado simulator for the low swirl ratio. At the higher swirl ratio though, the STD of tangential velocity is larger in Ward-type simulator. However, when $S=0.15$, the STD of tangential velocity exhibits completely different behavior with respect to with/without rotating downdraft. The STD of tangential velocity is close to zero at both elevations when the vortex is generated without rotating downdraft, but it presents very large values when the vortex is generated with rotating downdraft. A zero STD value implies a steady vortex at $S=0.15$ close to laminar flow,

$$h/R_{\max}=1.0.$$

which agrees with the vortex classification of Monji and Mitsuta (1985). However, the high STD value of tangential velocity does not necessarily indicate a high turbulent condition, because the vortex wander phenomenon discussed in the next session contributes simultaneously to the value of STD. Vortex wandering and turbulence are inter-related, more sophisticated data analyses are considered necessary to clarify the turbulence level.

3.2 Instantaneous tornado-like vortex structure

Fig. 10 compares the instantaneous axial vorticity on a horizontal plane ($h=50$ mm) for four simulations for two swirl ratios with/without the effect of rotating downdraft at $R=0.625$ m. Both flows shown in Figs. 10(a) and 10(b) obtained by the simulation at $S=0.74$ with/without the effect of rotating downdraft, respectively, can be characterized by multiple secondary vortices that rotate around a large vortex. These secondary vortices are highly turbulent and vary in size and position from time to time, as observed from the sequence of the vorticity snapshot. The vorticity concentrated at the vortex center forming a single vortex at $S=0.15$ for both Ward- and ISU-type simulators. However, the position of the single vortex center varies from time to time when the effect of rotating downdraft is included (ISU-type simulator), which is different from the case without the effect of rotating downdraft. The vortex in the Ward-type simulator is almost stationary, so the STD of tangential velocity is approximately zero at $S=0.15$.

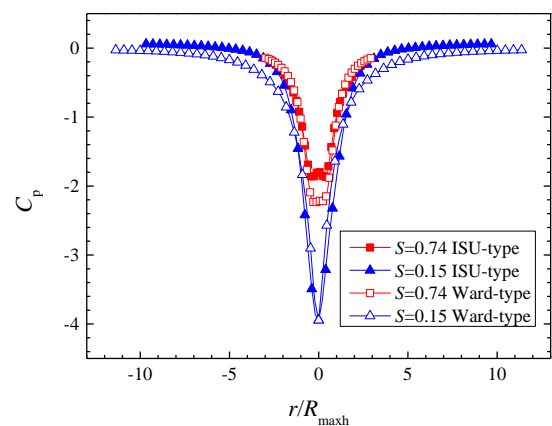


Fig. 8 Comparison of mean pressure coefficient profiles with/without downdraft at $h/R_{\max}=1.0$

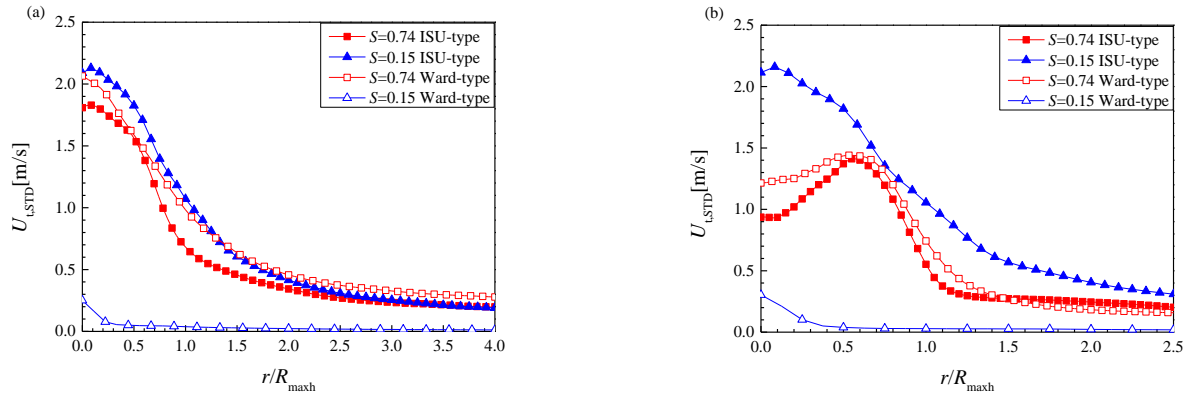


Fig. 9 Radial profile of standard deviation (STD) of tangential velocity, (a) $h/R_{max}=0.5$ and (b)

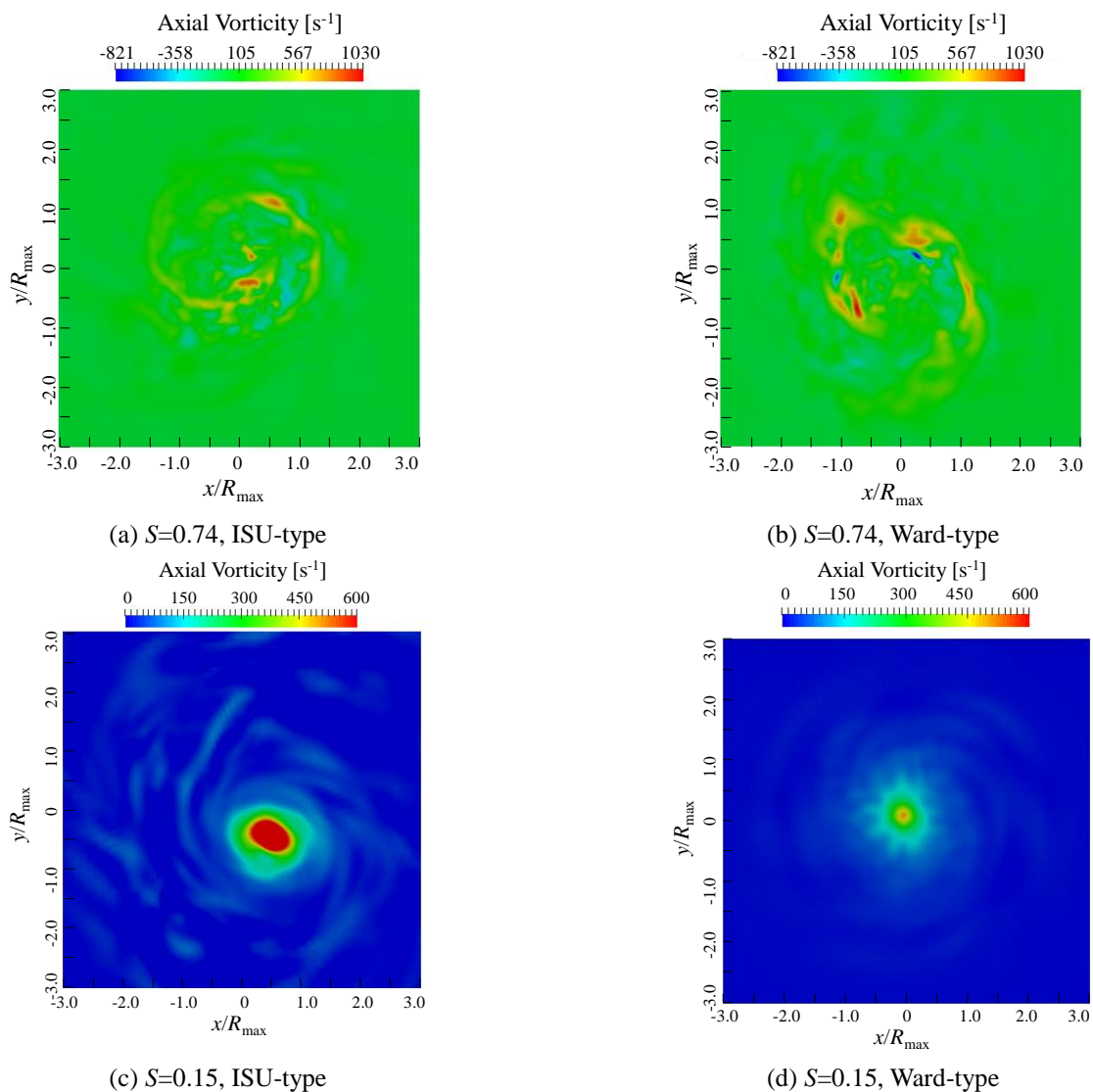


Fig. 10 Instantaneous axial vorticity fields on a horizontal plane

Fig. 11 compares snapshots of instantaneous radial vorticity in the meridian plane obtained by four simulations with different swirl ratios and with/without the effect of rotating downdraft at $R=0.625$ m. The rotating downdraft

has little influence on the magnitude and distribution of radial vorticity at swirl ratio $S=0.74$, but it significantly alters the radial vorticity field at swirl ratio $S=0.15$. The rotating downdraft continuously supplies horizontal

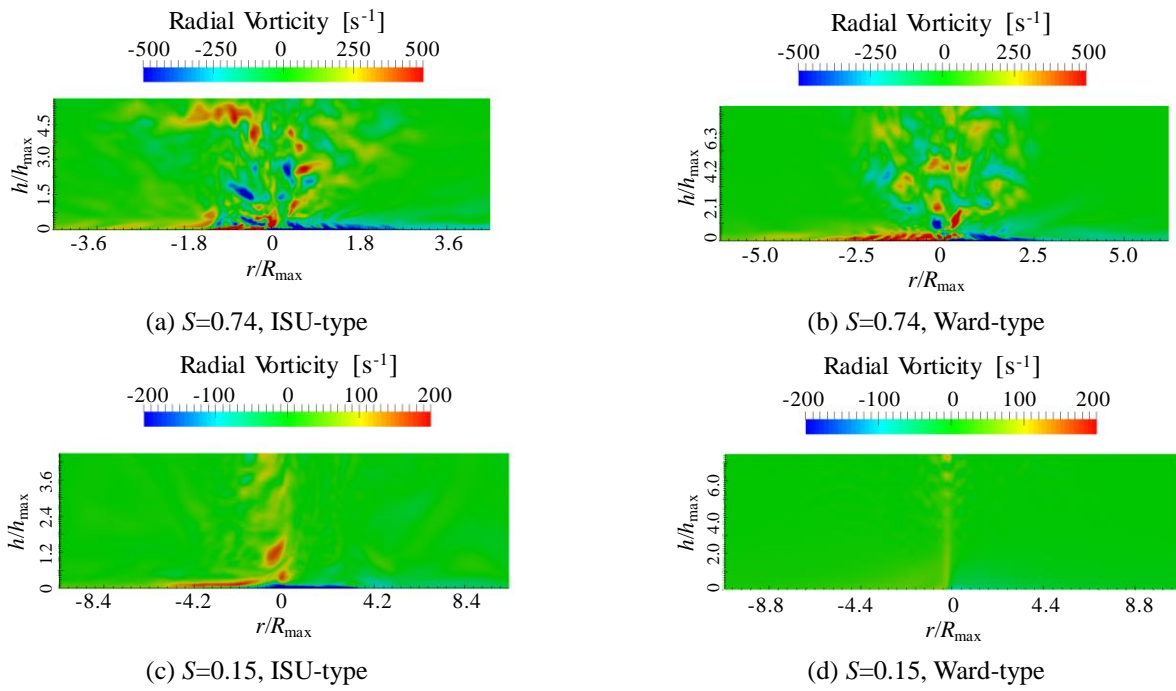


Fig. 11 Radial vorticity in meridian plane at different swirl ratios

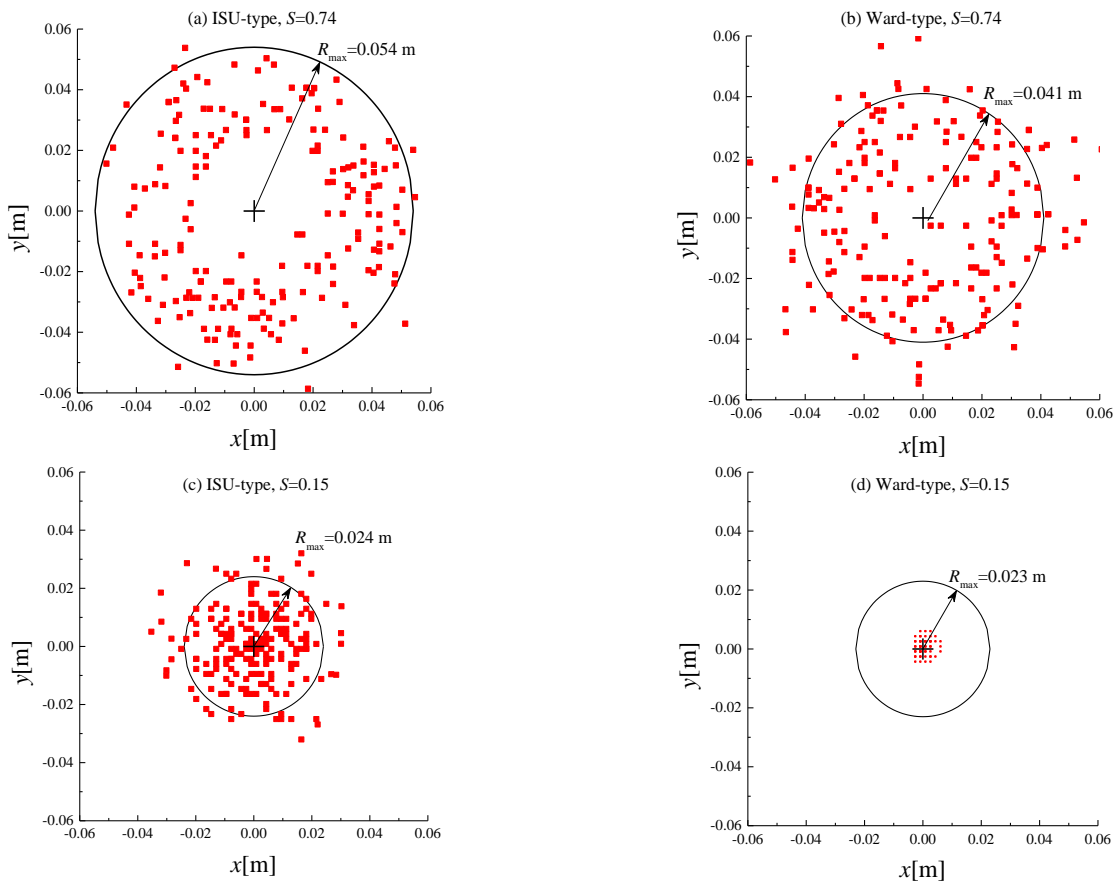


Fig. 12 Distribution of instantaneous vortex centers on a low horizontal plane ($h=50$ mm)

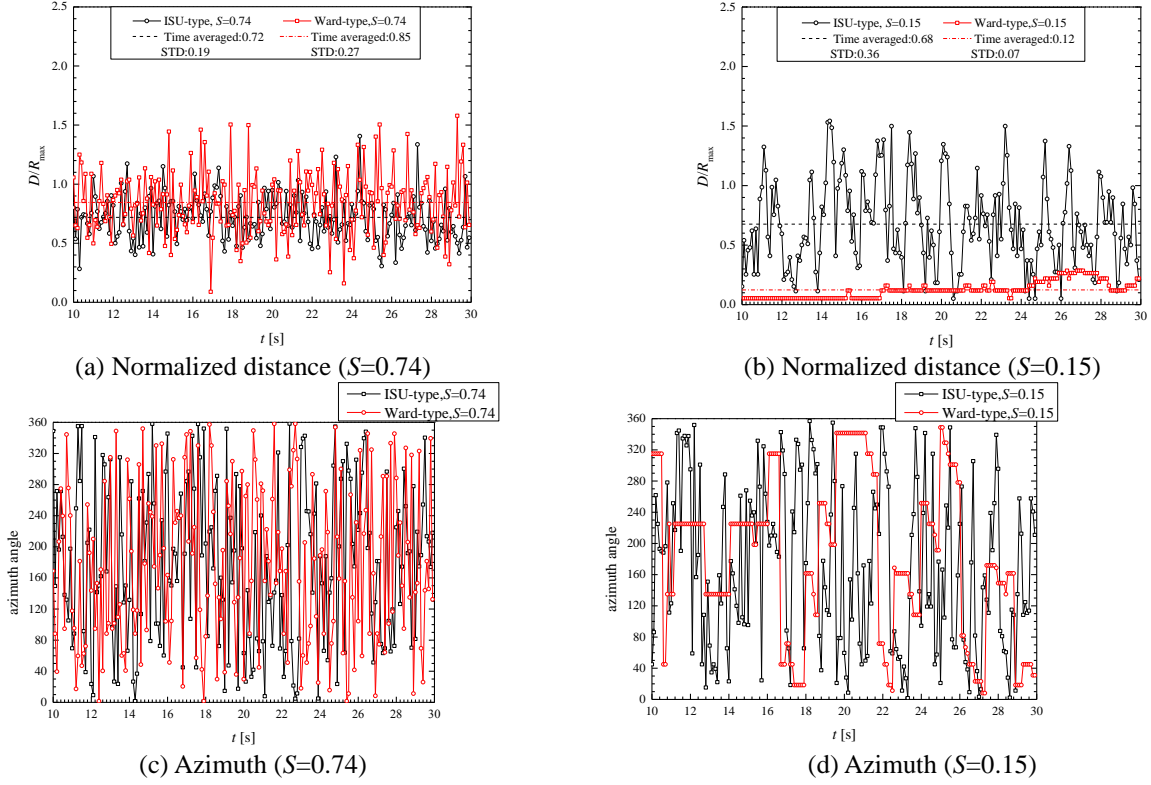


Fig. 13 Time histories of normalized distance and azimuth

vorticity into the convergence region, which may enhance the wander of a tornado-like vortex. At swirl ratio $S=0.15$, the vortex is basically stationary when there is no rotating downdraft (Fig. 11(d)). When the rotating downdraft is introduced, the stationary axial vortex wanders (Fig. 11(c)). However, at swirl ratio $S=0.74$, the vortex itself break down, forming multiple secondary vortices that rotate around a large vortex (Fig. 11(b)). The radial vorticity supplied from the rotating downdraft significantly affects the axial tornado-like vortices at the low swirl ratio.

Vortex wander has a direct connection with the multiple-cell vortex structure. As a concentrated negative pressure spot, the wander of a tornado-like vortex results in movement of both the minimum pressure point and the averaged pressure inside the vortex core. Due to its significant importance in both fundamentals and applications, the dependence of vortex wander on the tornado-like vortex generation mechanism needs to be investigated. The vortex center locations were thus quantitatively tracked. Considering the complexity of the multiple-cell vortex and the difference between the vortex structures of the single- and multiple-cell vortices, a definition of vortex center similar to Zhang and Sarkar (2012) is adopted in the present study. For the low-swirl-ratio single-cell vortex situation ($S=0.15$), the vortex center is defined as the location with the minimum in-plane pressure magnitude. For the high-swirl-ratio multiple-cell vortex situation ($S=0.74$), the vortex center is defined as the center of regions with pressure magnitude less than a given threshold considering the multiple secondary vortices.

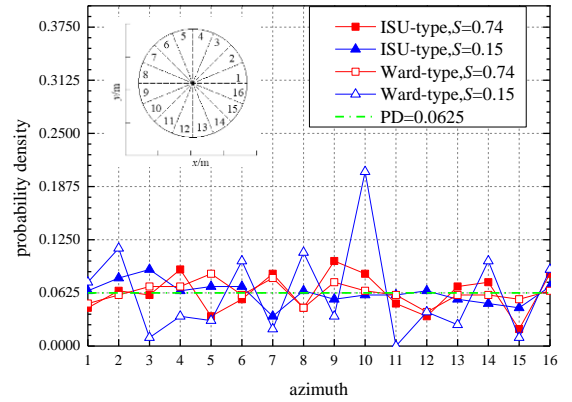


Fig. 14 Probability density of azimuth angle of the instantaneous vortex center

Fig. 12 compares the distribution of instantaneous vortex center locations on a low horizontal plane ($h=50$ mm) obtained at different swirl ratios ($S=0.15$ and 0.74) with/without rotating downdraft. The circle in Fig. 12 represents the vortex core at which the time-averaged tangential velocity reaches its maximum value on the horizontal plane ($h=50$ mm). This shows that vortex wander depends on both swirl ratio and the tornado generation mechanism. Figs. 12(a)-12(c) present uniformly distributed scatter of vortex center, while the instantaneous vortex center is very concentrated with respect to the vortex radius in Fig. 12(d), which is obtained when there is no effect of rotating downdraft at swirl ratio $S=0.15$. Fig. 12 shows that

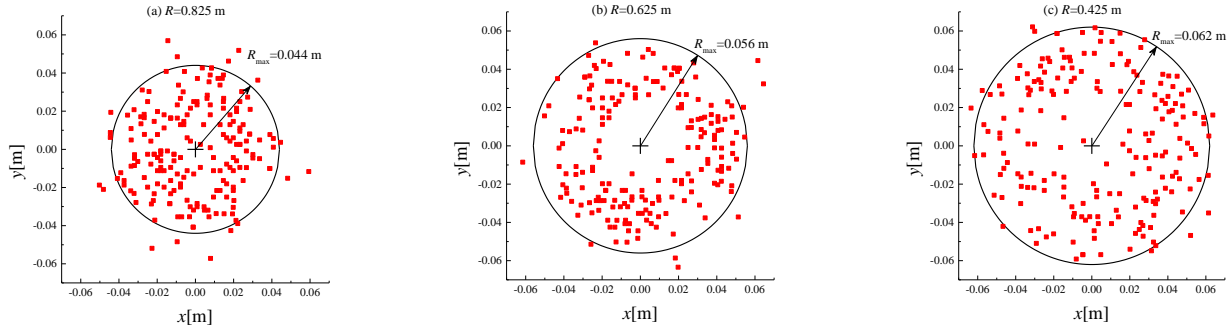
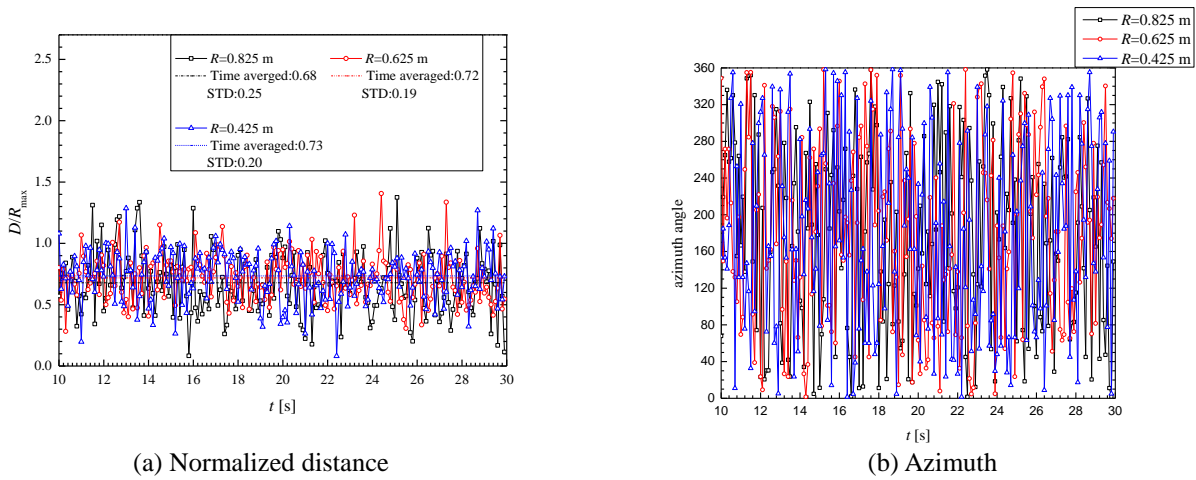


Fig. 15 Distribution of instantaneous vortex centers at different fetch lengths



(a) Normalized distance

(b) Azimuth

Fig. 16 Time histories of normalized distance and azimuth at different fetch lengths

the effect of rotating downdraft depends on the swirl ratio.

Figs. 13(a)-13(d) show the time histories of normalized distance (D/R_{\max}) and azimuth of instantaneous vortex center with respect to the simulator center respectively. It can be found that both of them vary randomly with time. At swirl ratio $S=0.74$, D/R_{\max} has averaged values of 0.72 and 0.85 and STD values of 0.19 and 0.27 respectively for the ISU-type and Ward-type simulators. Meanwhile, at swirl ratio $S=0.15$, D/R_{\max} has averaged values of 0.68 and 0.12 and STD values of 0.36 and 0.07 respectively for the ISU-type and Ward-type simulators. The obtained azimuth of instantaneous vortex center is further grouped into 16 azimuth angle. Fig. 14 shows the probability density of azimuth angle of instantaneous vortex center. It can be found that the tornado center is approximately equally distributed at 16 azimuth angles, except for the Ward-type simulator at a low swirl ratio $S=0.15$, in which the instantaneous vortex center concentrates around the simulator center thus the determination of vortex center contains uncertainty.

3.4 Fetch effect

Fetch length R may play important roles in determining the contribution of rotating downdraft to the tornado-like vortex structure. The dependence of the tornado-like-vortex

structure on fetch length for ISU-type simulators needs to be studied in order to enhance understanding of the effect of rotating downdraft. It is also important for optimizing the design of ISU-type simulators. Additional simulations are performed at fetch length $R=0.425$ m and 0.825 m in order to study fetch length effects. Some basic tornado parameters obtained for different fetch lengths are summarized in Table 1. Reynolds number is the same for all three simulations. Variations of swirl ratio, maximum tangential velocity and height where maximum tangential velocity occurs with fetch length are not clear. However, the vortex core radius shows a clear decrease with increase in fetch length.

Fig. 15 compares the distribution of instantaneous vortex center at different fetch lengths at height $h=50$ mm.

The core radius of the vortex is clearly influenced by the fetch length at this swirl ratio. The core radius of vortex decreases with increase in fetch length. It can be concluded that the fetch length of the rotating downdraft can be utilized as one parameter to design the diameter and scatter of the tornado-like vortex. Figs. 16(a) and 16(b) show the time histories of normalized distance (D/R_{\max}) and azimuth of instantaneous vortex center from the simulator center obtained at different fetch length respectively. Both distance and azimuth vary randomly with time without organized patterns. The averaged and STD values of normalized distance exhibit little change with fetch length. In addition,

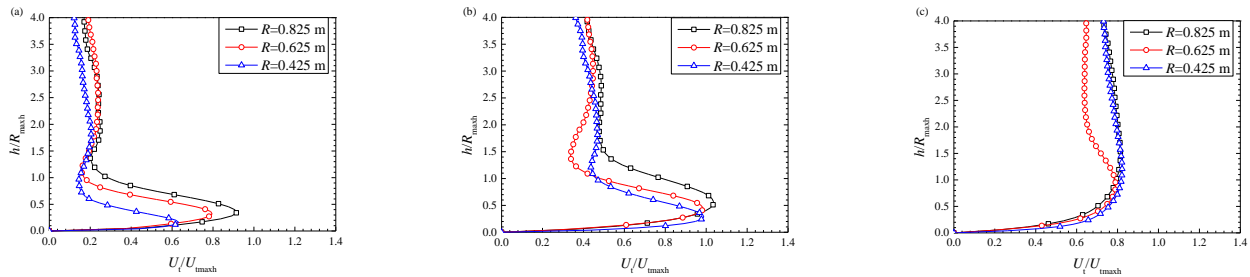


Fig. 17 Variation of vertical profile of tangential velocity with fetch length, (a) $r/R_{\max}=0.5$, (b) $r/R_{\max}=1.0$ and (c) $r/R_{\max}=2.0$

Fig. 17 shows the variation of vertical profile of tangential velocity with fetch length at three radial distances from the tornado-like-vortex center. It can be observed that the vertical profiles at a certain radial distance obtained at different fetch lengths maintain a similar tendency, although their values change. Fig. 17 also shows that the height at which the maximum tangential velocity in the vertical profile occurs increases with fetch length.

4. Conclusions

The effects of rotating downdraft on tornado-like-vortex dynamics were investigated systematically at two swirl ratios by large-eddy simulations. The present study showed that the dynamic vortex structure depends significantly on the vortex-generating mechanism, although the time-averaged structure remains similar. It was found that the rotating downdraft contributes to the vortex dynamics differently according to the value of swirl ratio, or in a more direct sense, according to whether the tornado-like vortex is single- or multiple-cell.

At a low swirl ratio, the rotating downdraft changes the vortex pattern from a one-cell structure to multiple secondary vortices that rotate around a large vortex. Thus, all three velocity components exhibit different spatial profiles, in which the axial velocity even changes with wind direction. However, at a high swirl ratio, rotating downdraft only slightly modifies the vortex characteristics. The normalized velocity profiles do not show significant change with/without rotating downdraft, although the size and velocity of the vortex vary. Meanwhile, vortex wander depends significantly on the rotating downdraft, which enhances the extent of vortex wander. In addition, the fetch length also modifies vortex features such as vortex size and velocity profiles.

Finally, it is noteworthy that it is difficult to judge whether a Ward- or ISU-type simulator is more appropriate for modelling a tornado for engineering applications because quantitative description of vortex dynamics such as the extent of vortex wander of real tornadoes still seems ambiguous. Also, the effect of rotating downdraft on vortex characteristics may vary when a tornado's translational speed is added into the study. However, we think the tornado-like vortex generated by ISU type simulator is closer to a real one because its swirl is created by rotating downdraft, which is one symbol of a tornado. A point worth emphasizing is that the present study revealed differences in

vortex characteristics due to the vortex generation mechanism, which should be carefully considered when they are used to investigate tornado-induced wind loads.

Acknowledgements

This research was funded by the National Natural Science Foundation of China (NSFC) Grant No. 51720105005 and 51478358, Cooperative Research Program of Civil Engineering College of Tongji University No. TMGFXK-2015-003 and Fundamental Research Funds for the Central Universities No. 22120170255.

References

- Cao, S. and Wang, J. (2013), "Statistical summary and case studies of strong wind damage in China", *J. Disaster Res.*, **8**(6), 1096-1102.
- Cao, S., Wang, J., Cao, J., Zhao, L. and Chen, X. (2015), "Experimental study of wind pressures acting on a cooling tower exposed to stationary tornado-like vortices", *J. Wind Eng. Ind. Aerod.*, **145**, 75-86.
- Chang, C.C. (1971), "Tornado wind effects on buildings and structures with laboratory simulation", *Proceedings of the 3rd International Conference on Wind Effects on Buildings and Structures*, Tokyo, Japan, 231-240.
- Church, C.R., Snow, J.T., Baker, G.L. and Agee, E.M. (1979), "Characteristics of tornado-like vortices as a function of swirl ratio: a laboratory investigation", *J. Atmos. Sci.*, **36**, 1755-1776.
- Haan, F.L., Balaramudu, V.K. and Sarkar, P.P. (2010), "Tornado-induced wind loads on a low-rise building", *Struct. Eng.*, **136**, 106-116.
- Haan, F.L., Sarkar, P., and Gallus, W.A. (2008), "Design, construction and performance of a large tornado simulator for wind engineering applications", *Eng. Struct.*, **30**, 1146-1159.
- Hu, H., Yang, Z., Sarkar, P. and Haan, F.L. (2011), "Characterization of the wind loads and flow fields around a gable-roof building model in tornado-like winds", *Exp Fluids*, **51**(3), 835-851.
- Ishihara, T., Oh, S. and Tokuyama, Y. (2011), "Numerical study on flow fields of tornado-like vortices using the les turbulence model", *J. Wind Eng. Ind. Aerod.*, **99**(4), 239-248.
- Kikitsu, H., Sarkar, P. and Haan, F.L. (2010), "Fundamental study on characteristics of tornado-induced wind load on low-rise building using a large tornado simulator", *Proceedings of the 21th National Symposium on Wind Engineering*, Tokyo, Japan, 149-154 (in Japanese).
- Kuai, L., Haan, F.L., Gallus, W.A. and Sarkar, P.P. (2008), "CFD simulations of the flow field of a laboratory simulated tornado

- for parameter sensitivity studies and comparison with field measurements”, *Wind Struct.*, **11**(2), 75-96.
- Lewellen, D.C., Lewellen, W.S. and Sykes, R.I. (1997), “Large-eddy simulation of a tornado's interaction with the surface”, *J. Atmos. Sci.*, **54**, 581-605.
- Liu, Z. and Ishihara, T. (2015), “Numerical study of turbulent flow fields and the similarity of tornado vortices using large-eddy simulations”, *J. Wind Eng. Ind. Aerod.*, **145**(2015), 42-60
- Liu, Z. and Ishihara, T. (2016), “Study of the effects of translation and roughness on tornado-like vortices by large-eddy simulations”, *J. Wind Eng. Ind. Aerod.*, **151**, 1-24.
- Mitsuta, Y. and Monji, N. (1984), “Development of a laboratory simulator for small scale atmospheric vortices”, *J. Natural Disaster Sci.*, **6**(1), 43-54.
- Monji, N. and Mitsuta, Y. (1985), “A laboratory experiment on the multiple structure in tornado-like vortices”, *Disaster Prevention Research Institute Annals, Kyoto University, No.26, B-1*, 427-436 (in Japanese).
- Natarajan, D. and Hangan, H. (2012), “Large eddy simulations of translation and surface roughness effects on tornado-like vortices”, *J. Wind Eng. Ind. Aerod.*, **104-106**, 577-584.
- Rotunno, R. (1977), “Numerical simulation of a laboratory vortex”, *J. Atmos. Sci.*, **34**, 1942-1956.
- Sabareesh, G.R., Matsui, M. and Tamura, Y. (2013), “Characteristics of internal pressures and net local roof wind forces on a building exposed to a tornado-like vortex”, *J. Wind Eng. Ind. Aerod.*, **112**, 52-57.
- Refan M. and Hangan H. (2017), “Surface pressures dependency on Reynolds number and swirl ratio in tornado vortices”, *Proceedings of the 13th Americas Conference on Wind Engineering*, May 21-24, 2017, Gainesville, Florida, USA.
- Tamura, Y. (representative). (2007), “Report of investigation of serious tornado damage in Saroma-cho, Hokkaido”, *Grant-in-Aid for Scientific Research* (in Japanese).
- Wang, J., Cao, S., Pang, W. and Cao, J. (2017), “Experimental study on effects of ground roughness on flow characteristics of tornado-like vortices”, *Bound.-Lay. Meteorol.*, **162**(2), 319-339.
- Wang, J., Cao, S., Pang, W. and Cao, J. (2018), “Experimental study on tornado-induced wind pressures on a cubic building with openings”, *J. Struct. Eng. - ASCE*, in press.
- Ward, N.B. (1972), “The exploration of certain features of tornado dynamics using a laboratory model”, *J. Atmos. Sci.*, **29**, 1194-1204.
- Zhang, W. and Sarkar, P. (2012), “Near-ground tornado-like vortex structure resolved by particle image velocimetry (PIV)”, *Exp. Fluids*, **52**, 479-493.